

## Plasma Instability at the Inner Edge of the Accretion Disk—II

S. C. Tripathy, *Udaipur Solar Observatory, Physical Research Laboratory, 11, Vidya Marg, Udaipur, 313001*

C. B. Dwivedi, *Institute of Advanced Study in Science and Technology, Khanapara, Guwahati, 781022*

A. C. Das & A. R. Prasanna *Physical Research Laboratory, Navrangpura, Ahmedabad 380 009*

Received 1993 January 26; accepted 1993 May 17

**Abstract.** A two-dimensional instability analysis for a magneto-keplerian disk flow around a compact object is presented here. Using the eigenvalue technique, linearly coupled perturbed equations have been numerically solved within the local approximation. It is concluded that Kelvin-Helmholtz, magnetosonic (fast and slow) and resistive electromagnetic modes exist. However, only the magnetosonic mode can destabilise the disk structure. Further, we discuss the properties of different modes as a function of disk parameters and plot the eigenmode structures for different physical quantities.

*Key words:* Accretion disks—hydromagnetics—instability

### 1. Introduction

As is well known, the accretion disk models have been very popular in the context of radiation emission and energetics associated with high energy astrophysical sources. In this context there have been several studies of the dynamics of disks mostly without the electromagnetic fields while some have considered self consistent electromagnetic fields for plasma disks (Prasanna 1991 and references therein). Recently, we (Tripathy *et al.* 1990) have considered the equilibrium structure of a plasma disk around a compact object including the gravitational field of the central source and have solved the MHD equations self-consistently. From the turning point behaviour observed in the pressure profiles it was conjectured that there could exist plasma instabilities at the inner edge of such disks. This was the point of investigation in a subsequent paper (Tripathy *et al.* 1993, hereinafter referred to as paper I) wherein we considered one-dimensional radial perturbation analysis under local approximation. This had revealed the existence of Kelvin-Helmholtz (KH), resistive-electromagnetic (RE) and magnetosonic (MS) modes. However, only the magnetosonic mode is found to be unstable and it was concluded that only this mode could destabilise the disk structure.

The present study is an extension of the above work which includes the perturbation in azimuthal direction also. From this two-dimensional perturbation analysis we find that the magnetosonic mode is still unstable and the other two modes are stable. However, the finite azimuthal perturbation causes the excitation of the slow magnetosonic (SMS) mode which was absent in the case of the purely radial perturbation.

Using numerical techniques, we have also studied the propagation characteristics of fast and slow magnetosonic modes and their growth rates as a function of different plasma parameters.

The plan of the paper is as follows. The formalism and the general description of the eigenvalue technique are outlined in section 2. Section 3 outlines the basic perturbation equations and the results are discussed in section 4. Finally, section 5 summarises the conclusions.

## 2. Formalism

In this section, we carry out a detailed stability analysis of the equilibrium configuration given by Tripathy *et al.* (1990). The basic linear perturbation equations for this problem are already given in paper I (Equations 2.1 to 2.15). Following the Standard normal mode analysis, the general time dependent perturbations are written as

$$\tilde{\Psi}(r, \theta, \phi, t) = \tilde{\psi}(r) \exp[i(\nu t + n\theta + m\phi)], \quad (2.1)$$

where  $n$  is the meridional mode number,  $m$  is the azimuthal mode number signifying the number of azimuthal crests around a circumference of radius  $r$ ,  $\nu$  is the frequency which may be complex and  $\tilde{\psi}(r)$  is the amplitude of the perturbation which is also complex. For the sake of simplicity and for an analytical understanding of the nature of the instabilities, the stability analysis is performed at the  $\theta = \pi/2$  plane. Since, the plasma motion at the inner boundary in the equilibrium configuration was found to be primarily along the azimuthal direction, we further assume the flow to be along the azimuthal direction only ( $V_\phi \neq 0$ ;  $V_r, V_\theta = 0$ ).

### 2.1 Eigenvalue Techniques

The numerical method to solve any given set of equations by the method of eigenvalue techniques consists of converting the system of linearised equations into the form of an algebraic matrix eigenvalue problem (Simonutti 1976)

$$(A_r + iA_i)X = \lambda (B_r + iB_i)X, \quad (2.2)$$

where  $A$  and  $B$  are complex square matrices of finite dimension  $n$  and its elements are defined in terms of the independent variables of the problem.  $X$  is a column vector of dimension  $n$  and  $\lambda$  is a scalar and each of these quantities may be complex. It is well known that the eigenvalue will represent the dependant variable of the dispersion relation and the elements of the eigenvector will represent the selected dynamic variables of the system. With this formulation it is possible to directly determine the solutions of the dispersion relation by calculating the eigenvalue and the eigenvectors. The eigenvectors contain information concerning the nature of the dynamic variables i.e. polarizations etc. for each mode of oscillations.

To obtain the eigenvalues and eigenvectors of the complex matrix numerically, we use the routines from the EISPAK package (Smith *et al.* 1974). However, this package contains subroutines which solve an eigenvalue problem of the type

$$(A_r + iA_i)X = \lambda (B)X, \quad (2.3)$$

where the matrix  $B$  is real. In order to achieve this, we assume the time dependence of the perturbation to be  $vt$  instead of  $ivt$  where  $v$  is still the complex frequency. With this new notation, positive  $v_r$ , the real part of  $v$  indicates growing solution and implies the system to be unstable. Similarly  $v_i$ , the imaginary part of the frequency represents the dispersion characteristics of the wave.

## 2.2 Basic Equations

We consider small perturbations of any physical quantity  $\Psi$  as  $\Psi = \psi + \tilde{\psi}$ , where  $\psi$  is the equilibrium part and  $\tilde{\psi}$  is the generic perturbation such that  $\tilde{\psi}/\psi \ll 1$ . Expressing the time dependent perturbations as

$$\tilde{\Psi}(r, \phi, t) = \tilde{\psi}(r) \exp[(vt + im\phi)], \quad (2.4)$$

the basic linearised equations can be represented as follows:

$$\frac{v}{c} \tilde{E}_r + \frac{im}{r} \tilde{B}_\theta + \frac{4\pi\sigma}{c^2} [c\tilde{E}_r - B_\theta \tilde{V}_\phi - V_\phi \tilde{B}_\theta] = 0, \quad (2.5)$$

$$\frac{v}{c} \tilde{E}_\theta + \frac{d\tilde{B}_\phi}{dr} + \frac{\tilde{B}_\phi}{r} - \frac{im}{r} \tilde{B}_r + \frac{4\pi\sigma}{c^2} [c\tilde{E}_\theta + V_\phi \tilde{B}_r] = 0, \quad (2.6)$$

$$\frac{v}{c} \tilde{E}_\phi - \frac{1}{r} \frac{d\tilde{B}_\theta}{dr} - \tilde{B}_\theta + \frac{4\pi\sigma}{c^2} [c\tilde{E}_\phi + B_\theta \tilde{V}_r] = 0, \quad (2.7)$$

$$\frac{v}{c} \tilde{B}_r - \frac{im}{r} \tilde{E}_\theta = 0, \quad (2.8)$$

$$\frac{v}{c} \tilde{B}_\theta - \frac{\tilde{E}_\phi}{r} - \frac{d\tilde{E}_\phi}{dr} + \frac{im}{r} \tilde{E}_r = 0, \quad (2.9)$$

$$\frac{v}{c} \tilde{B}_\phi + \frac{\tilde{E}_\theta}{r} + \frac{d\tilde{E}_\theta}{dr} = 0, \quad (2.10)$$

$$v\tilde{V}_r + \frac{(im-2)}{r} V_\phi \tilde{V}_\phi + \frac{1}{\rho} \frac{d\tilde{P}}{dr} - \frac{1}{\rho^2} \frac{dP}{dr} \tilde{\rho} + \frac{1}{c\rho} [-B_\theta \tilde{J}_\phi - \tilde{B}_\theta J_\phi + \tilde{E}_r J_t] - \frac{\tilde{\rho}}{c\rho^2} [E_r J_t - B_\theta J_\phi] = 0, \quad (2.11)$$

$$\left( v + \frac{im}{r} V_\phi \right) \tilde{V}_\theta = 0 \quad (2.12)$$

$$v\tilde{V}_\phi + \frac{im}{r} V_\phi \tilde{V}_\phi + \left( \frac{V_\phi}{r} + \frac{dV_\phi}{dr} \right) \tilde{V}_r + \frac{im}{\rho r} \tilde{P} + \frac{1}{c\rho} [B_\theta \tilde{J}_r + \tilde{E}_\phi J_t] = 0. \quad (2.13)$$

$$\left( v + \frac{imV_\phi}{r} \right) \tilde{\rho} + \rho \left[ \frac{d\tilde{V}_r}{dr} + \frac{im}{r} \tilde{V}_\phi + \frac{2\tilde{V}_r}{r} \right] = 0. \quad (2.14)$$

$$\tilde{J}_r = -\frac{\sigma}{c} [c\tilde{E}_r - \tilde{B}_\theta V_\phi - B_\theta \tilde{V}_\phi] \quad (2.15)$$

$$\tilde{J}_\theta = -\frac{\sigma}{c} [c\tilde{E}_\theta + \tilde{B}_r V_\phi] \quad (2.16)$$

$$\tilde{J}_\phi = -\frac{\sigma}{c}[c\tilde{E}_\phi + B_\theta\tilde{V}_r] \quad (2.17)$$

$$\tilde{J}_r = -\frac{\sigma}{c}[E_r\tilde{V}_r + \tilde{E}_\phi V_\phi] \quad (2.18)$$

As for the energy equation, we use the adiabatic law (paper I)

$$\frac{d}{dt}[P\rho^{-\gamma}] = 0, \quad (2.19)$$

Here the notations have their usual meanings.

### 3. Local analysis

The approach of local analysis which is a well-established procedure in the studies of plasma instabilities assumes the wavelength ( $\lambda$ ) of the perturbation to be small compared to the scale size of the equilibrium inhomogeneity in the system. For example, if one assumes the scale size to be the pressure scale length  $\left(L_p^{-1} = \frac{1}{P} \frac{dP}{dr}\right)$ ,

then the local approximation demands that  $kL_p \gg 1$ , where  $k$  is the radial wave number and implies that the space variation of the amplitude of the perturbation over its scale length is negligible. In addition, a local analysis allows one to Fourier transform the perturbed variables even in the direction of inhomogeneity (Rognlien & Weinstock 1974). Thus the perturbed quantities along the radial direction can be expressed as  $\tilde{\psi}(r) = \tilde{\psi} \exp [ikr]$ . As a result the differential Equations (2.5) to (2.18) are transformed into the algebraic equations which are to be solved by appropriate method. Defining the dimensionless variables,  $\tilde{E}_i = \frac{\tilde{E}_i}{B_\theta}$ ,  $\tilde{B}_i = \frac{\tilde{B}_i}{B_\theta}$ ,  $\tilde{V}_i = \frac{\tilde{V}_i}{c}$ ,  $k = \kappa R$ ,  $\alpha = r/R$ ,  $\hat{\sigma} = 4\pi\sigma R/c$ ,  $\omega = \nu R/c$ ,  $\hat{V}_A^2 = \frac{B_\theta^2}{4\pi\rho c^2}$ ,  $\hat{C}_s^2 = \frac{\gamma P}{\rho c^2}$ , the linearised perturbation equations in dimensionless form are written as

$$(\omega + \hat{\sigma})\tilde{E}_r + \frac{im}{\alpha}\tilde{B}_\theta - \hat{\sigma}\tilde{V}_\phi - \hat{\sigma}\hat{V}_\phi\tilde{B}_\theta = 0, \quad (3.1)$$

$$(\omega + \hat{\sigma})\tilde{E}_\theta + \left(ik + \frac{1}{\alpha}\right)\tilde{B}_\phi + \left(\hat{\sigma}\hat{V}_\phi - \frac{im}{\alpha}\right)\tilde{B}_r = 0, \quad (3.2)$$

$$(\omega + \hat{\sigma})\tilde{E}_\phi - \left(ik + \frac{1}{\alpha}\right)\tilde{B}_\theta + \hat{\sigma}\tilde{V}_r = 0, \quad (3.3)$$

$$\omega\tilde{B}_r - \frac{im}{\alpha}\tilde{E}_\theta = 0, \quad (3.4)$$

$$\omega\tilde{B}_\theta + \frac{im}{\alpha}\tilde{E}_r - \left(ik + \frac{1}{\alpha}\right)\tilde{E}_\phi = 0, \quad (3.5)$$

$$\omega\tilde{B}_\phi + \left(ik + \frac{1}{\alpha}\right)\tilde{E}_\theta = 0, \quad (3.6)$$

$$\begin{aligned}
 & (\omega + \hat{\sigma} \hat{V}_A^2) \tilde{V}_r + \frac{(im - 2)}{\alpha} \hat{V}_\phi \tilde{V}_\phi + \hat{\sigma} \hat{V}_A^2 \tilde{E}_\phi \\
 & + \left( \frac{(\gamma - 1) dP}{\rho c^2 d\alpha} \right) \tilde{\rho} + \hat{C}_s^2 \frac{d\tilde{\rho}}{d\alpha} = 0,
 \end{aligned} \tag{3.7}$$

$$\left( \omega + \frac{im}{\alpha} \right) \tilde{V}_\theta = 0, \tag{3.8}$$

$$\omega \tilde{V}_\phi + \left( \frac{im}{\alpha} \hat{V}_\phi + \hat{\sigma} \hat{V}_A^2 \right) \tilde{V}_\phi - \hat{\sigma} \hat{V}_A^2 (\tilde{E}_r - \hat{B}_\theta \tilde{V}_\phi) + \hat{C}_s^2 \frac{im}{\alpha} \tilde{\rho} = 0, \tag{3.9}$$

$$\left( \omega + \frac{im}{\alpha} \hat{V}_\phi \right) \tilde{\rho} + \left( \frac{2}{\alpha} + ik \right) \tilde{V}_r + \frac{im}{\alpha} \hat{\rho} \tilde{V}_\phi = 0. \tag{3.10}$$

Here  $\tilde{V}_A$  and  $\hat{C}_s$  represent the normalised Alfvén and sound speeds respectively and the hat denotes the normalised quantities. In subsequent analysis, as there is no more ambiguity the hat over the quantities are dropped.

#### 4. Results and discussions

In order to check the consistency of the results with that obtained in paper I by the method of complex roots, the set of linearised equations are solved again by the eigenvalue formalism. These are obtained by setting  $m = 0$  in Equations (3.1 – 3.10). As mentioned earlier, we use the numerical routines from the EISPAK package (Smith *et al.* 1974). Below we first describe the results of this analysis briefly and in the next section we discuss the results of the two-dimensional analysis.

##### 4.1 One-dimensional Analysis

As mentioned in paper I for purely radial perturbations, the perturbed magnetic field along the radial direction ( $B_r$ ) and the perturbed velocity along the meridional direction ( $V_\theta$ ) are zero. This reduces the number of equations as well as the number of variables by two. The remaining eight equations constitute an eigenvalue problem. However, for better numerical results, the Equations (3.2) and (3.6) are grouped together. The remaining six equations form another group. These two sets are then solved separately as two different eigenvalue problems. The numerical computations of the total sets show the presence of two stable and one unstable mode. From the study of the eigenvalues with different physical parameters the three different modes are identified as K-H, magnetosonic and RE modes. Since the value of  $\omega_r$  for magnetosonic mode is positive, it is concluded that only the magnetosonic mode is unstable. As a comparison, the growth rate of the magnetosonic mode obtained by two different methods as outlined above is plotted in Fig. 1. It can be clearly seen that the results obtained by the eigenvalue formalism match very well with the calculations carried out in paper I by the method of finding the complex roots. The added advantage of this method is to obtain the eigenvectors of different modes. Fig. 2 represents the eigenmode structure of the MS mode. The mode structures as

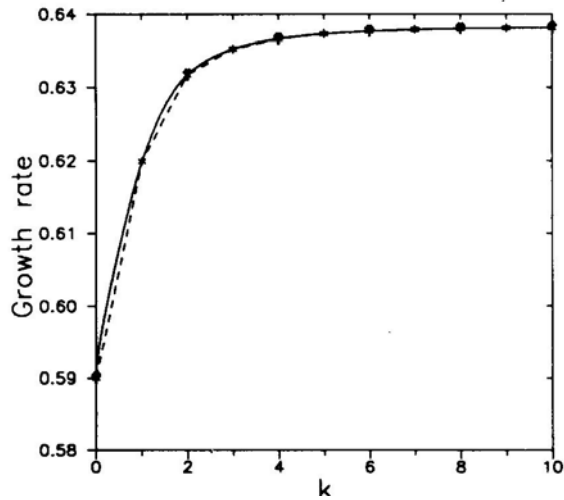


**Figure 1.** Comparison of the normalised growth rate for the magnetosonic mode by two different methods viz. (a) method of finding complex roots (solid line) (b) eigenvalue techniques (-\*-\*)

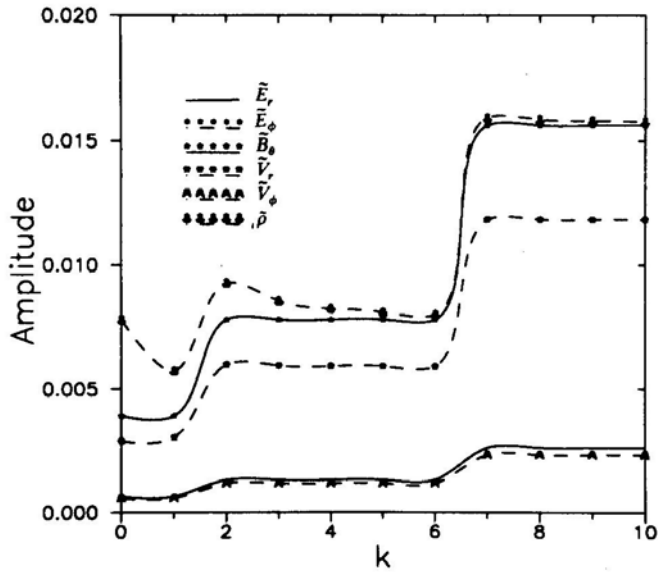


**Figure 2.** Eigenmode structures of the magnetosonic mode for purely radial perturbation obtained by using the eigenvalue technique.

a function of  $k$  give the distribution of energy over the possible wavelengths and from this figure, it is clear that the energy is distributed over the long wavelengths.

#### 4.2 Two-dimensional Analysis

Having checked the consistency of the eigenvalue technique as outlined above, we next carry out the two-dimensional perturbation analysis using the same subroutines.

As explained in paper I and again outlined above, we separate the complete set of Equations (3.1–3.10) into two groups and solve them separately in order to obtain better numerical results. Thus, Equations (3.2), (3.4) and (3.6) constitute one eigenvalue problem while the remaining seven equations with seven variables from the second eigenvalue problem.

The study of the first problem in the framework of the eigenvalue analysis reveals the existence of RE mode with complex  $\omega$  and is purely electromagnetic in nature. This mode propagates radially inward and its eigenvalue becomes purely real for higher  $m$  values ( $m \geq 2$ ). However, this mode is found to be stable within our assumptions. However, we conjecture that the mode may be modified if the finite thickness of the accretion disk is taken into account. A similar result was reported by Miura & Pritchett (1982).

The analyses of the second set of equations by the method of the eigenvalue techniques reveal the existence of three basic modes viz. Kelvin-Helmholtz and fast

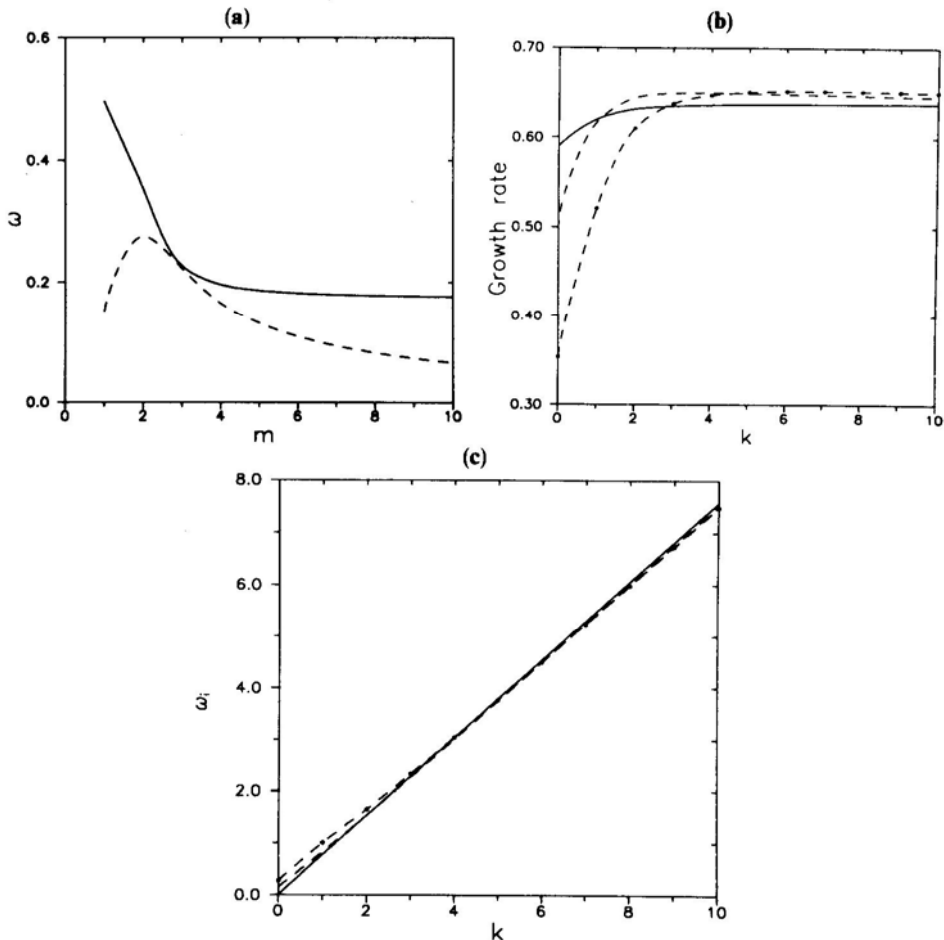


**Figure 3.** (a) The normalised growth rate (dashed line) and the normalised dispersion curve (solid line) for purely azimuthal perturbation ( $k = 0$ ) for fast magnetosonic wave, (b) Normalised growth rate and (c) Normalised dispersion curve of the same mode with  $m$  as a parameter,  $m = 0$  (solid line),  $m = 1$  (dashed line),  $m = 2$  (-★-★).

and slow magnetosonic modes. However only the magnetosonic modes were found to be unstable by its positive growth rates. The presence of the slow magnetosonic mode in this particular two-dimensional analysis clearly manifests the importance of the inclusion of the perturbations along the azimuthal direction.

The growth rates and dispersion curves of these two modes as a function of  $m$  and  $k$  are given in Figs. 3 and 4. The phase velocity calculation of slow and fast magnetosonic modes show the direction of propagation of these waves and it is found that the waves propagate in directions opposite to each other. For purely azimuthal perturbation ( $k = 0$ ) the slow mode propagates along the flow while the fast one propagates in a direction opposite to the plasma flow. However, the rates at which FMS grows is higher than SMS. The effect of higher  $m$ -mode numbers on these instabilities can be clearly seen from these figures and it is concluded that higher  $m$  values enhance the growth rates of the magnetosonic modes. The figures further reveal that these waves with a purely azimuthal propagation achieve asymptotically constant growth rate for higher  $m$  values. Thus we can stress that the addition of perturbation along the azimuthal direction introduces a stabilizing effect into the

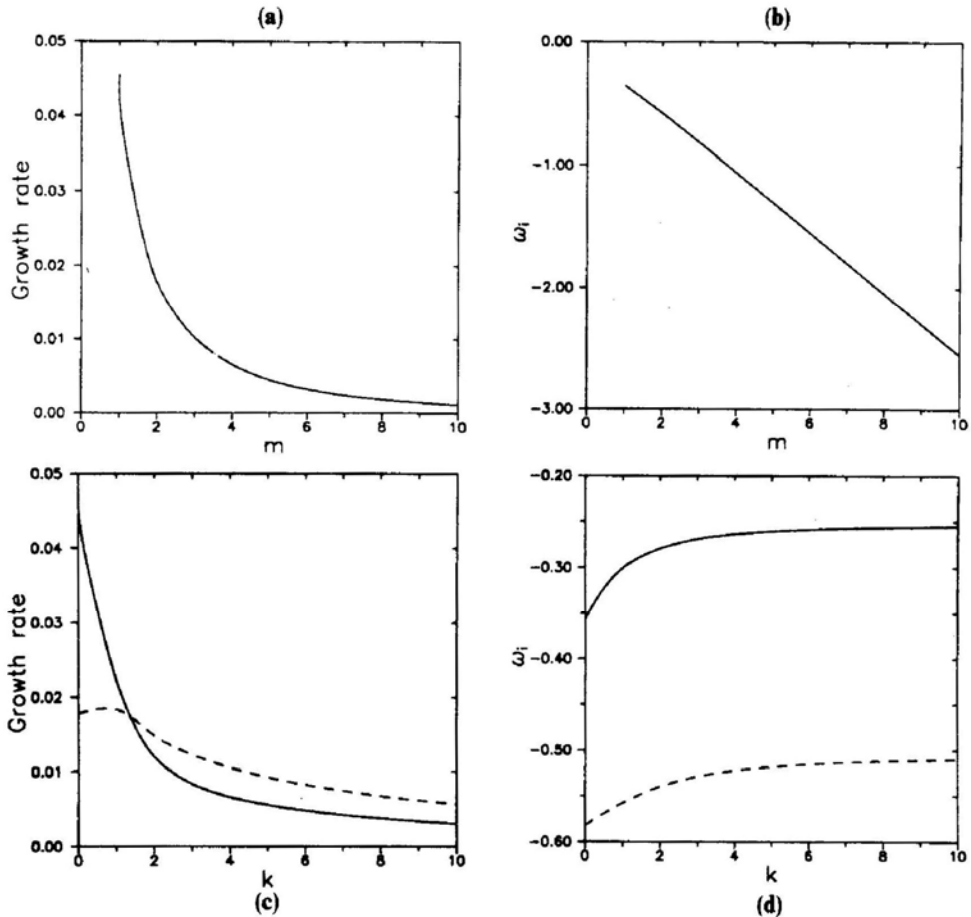


**Figure 4.** (a) The normalised growth rate and (b) Normalised dispersion curve for a purely azimuthal ( $k = 0$ ) slow magnetosonic mode, (c) Normalised growth rate and (d) Normalised dispersion curve of the mode with  $m$  as a parameter,  $m = 1$  (solid line),  $m = 2$  (dashed line).

system. This nature of the growth rate is in qualitative agreement with the work of Miura & Pritchett (1982) where they find that the growth rate is reduced due to the stabilizing effects of the finite value of  $k_z$ , where  $k_z$  is the perturbation along the  $z$  direction in cylindrical coordinate system. The investigation of the dispersion characteristics of these modes reveal that the FMS modes are non-dispersive along the radial direction (Fig. 3c) but dispersive in azimuthal direction (Fig 3a). Contrary to this, the SMS modes are weakly dispersive along radial direction (Fig.4d) and non-dispersive in azimuthal direction (Fig. 4b).

We have also analysed the properties of these two magnetosonic modes as a function of disk parameters viz. Alfvén velocity  $V_A$ , sound speed  $C_s$  and azimuthal velocity  $v_\phi$ . The growth rates of these instabilities are found to be higher for subsonic (Fig. 5) and sub-Alfvénic (Fig. 6) plasma flows. The analysis further demonstrates that the fast (slow) mode depends on  $V_A(C_s)$  and the instability is switched off for zero value of these parameters. However, these modes are weakly dependent on the value

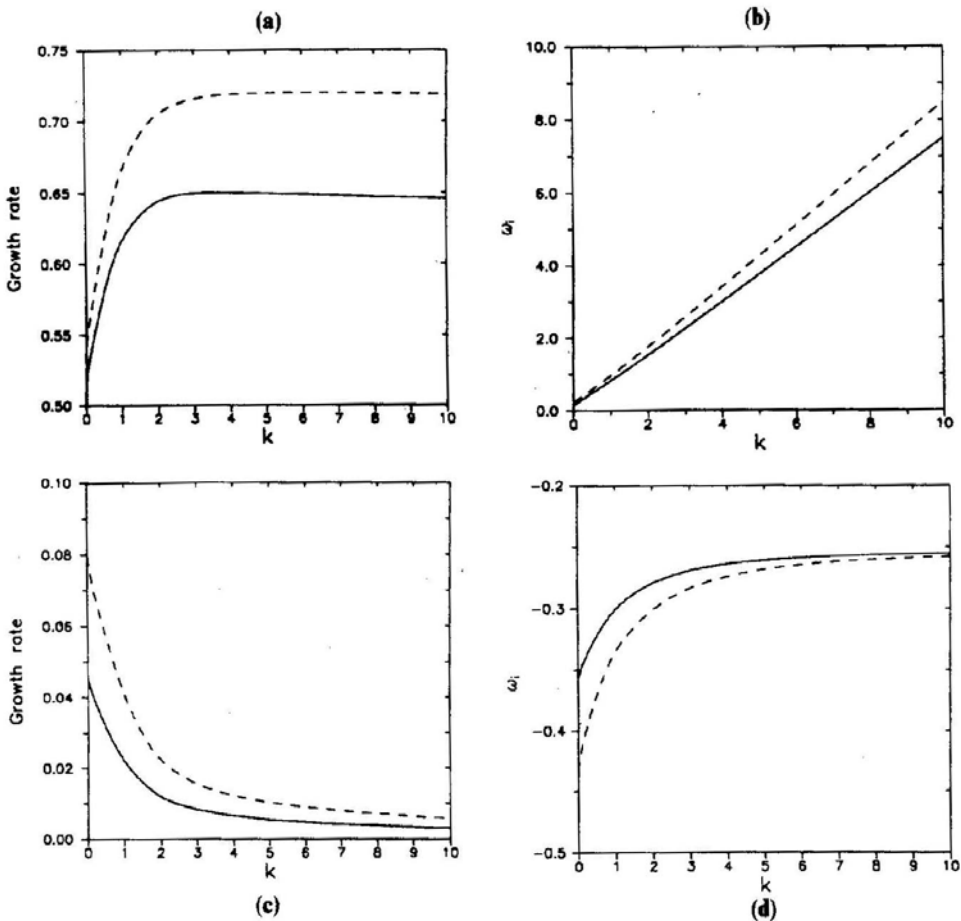


**Figure 5.** (a) The normalised growth rate and (b) Normalised dispersion curve of the fast magnetosonic mode for different sound speed for  $m = 1$ . Figures (c) and (d) respectively represent the same curves for SMS mode. In all these figures  $C_s$  (normalised) = 0.4394 is represented by the solid line and  $C_s$  (normalised) = 0.7 is represented by the dashed line.

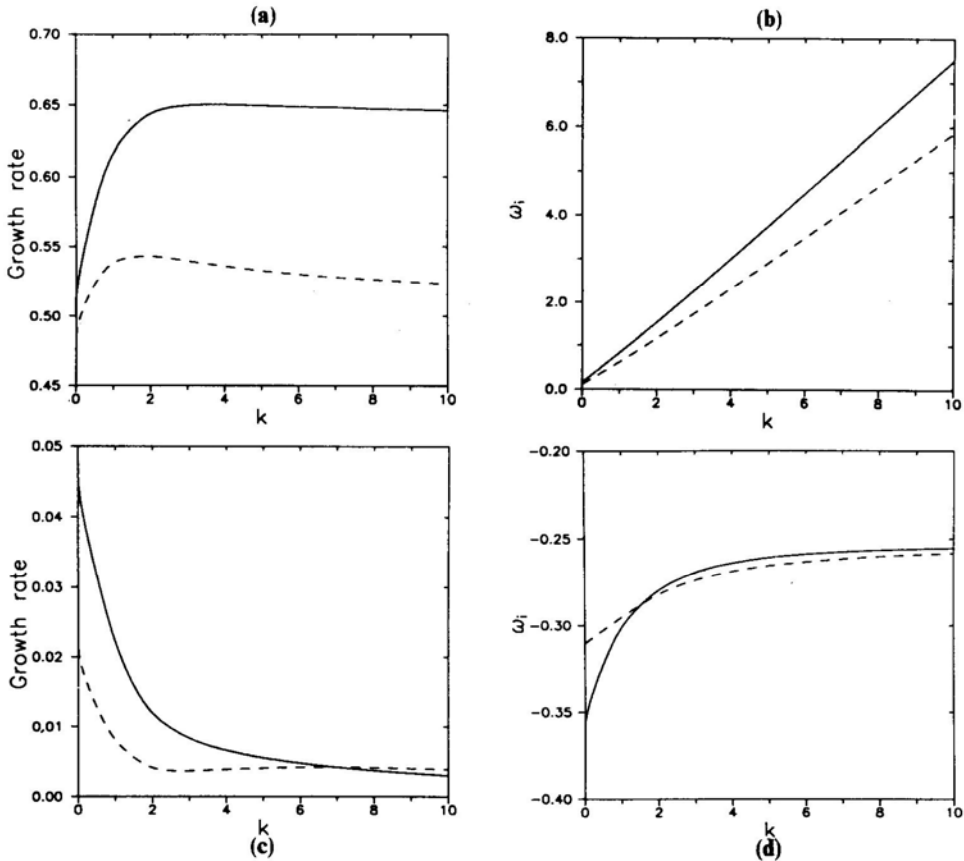


**Figure 6.** (a) The normalised growth rate and (b) Normalised dispersion curve for different Alfvén velocity  $V_A$  for FMS mode. Figures (c) and (d) respectively represent the same curves for SMS mode. All these curves are plotted with  $m = 1$ ,  $V_A = 0.942$  (solid line) and  $V_A = 0.5$  (dashed line).

of  $V_\phi$  (Fig. 7) and exist even for a static case ( $V_\phi = 0$ ). In addition MS modes are found to be independent of the finite conductivity of the fluid.

We now turn to the discussion of the eigenmode structures of these instabilities. Fig. 8 shows the amplitudes of perturbed electric, magnetic, velocity and density fields as a function of  $m$  with the normalised parameters  $V_\phi = 0.316$ ,  $V_A = 0.942$  and  $C_S = 0.4394$ . The amplitude of density perturbation of these two instabilities has a broad maximum which falls off monotonically with a higher mode number. However, the decreasing rate is different for both the modes. It is worthwhile to note that for a given instability, the distribution of the amplitudes of all the fields and the corresponding growth rates as a function of wave number have identical patterns. This matching is expected and as a result we emphasize that the analysis is consistent.

## 5. Conclusion

In this paper, we have carried out a two-dimensional stability analysis of a magnetofluid at the inner edge of the accretion disk around a compact object. This

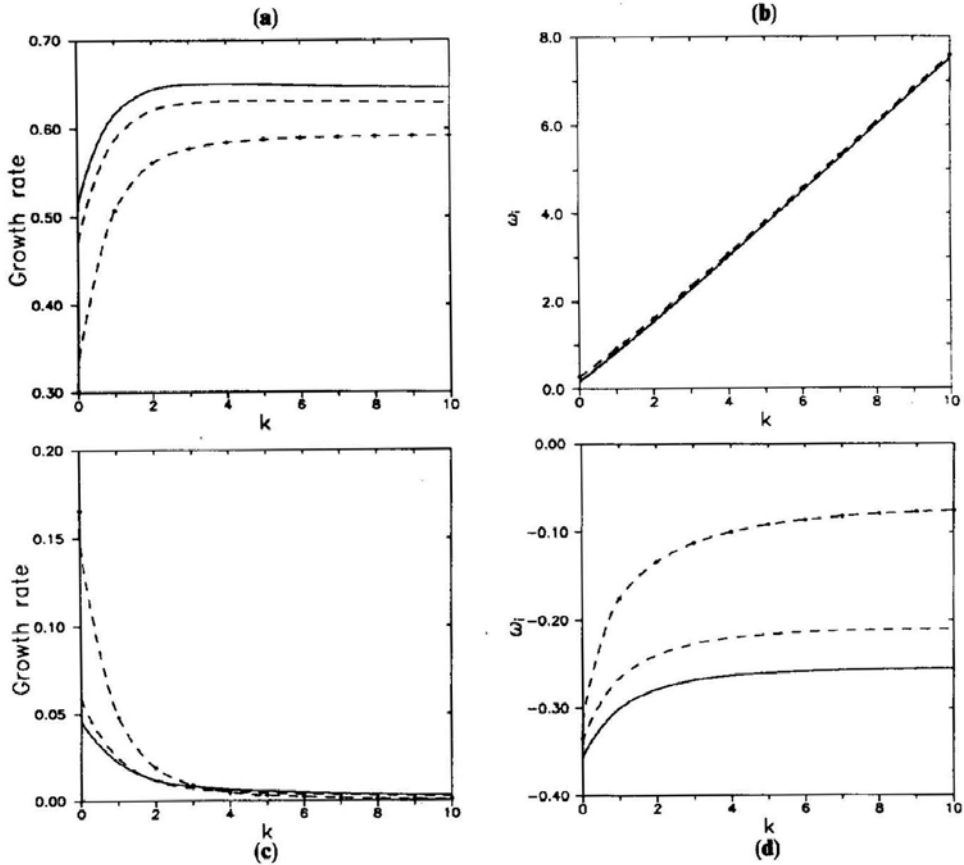


**Figure 7.** (a) The normalised growth rate and (b) Normalised dispersion curve for different azimuthal velocity  $V_\phi$  for FMS mode. Figures (c) and (d) respectively represent the same curves for SMS mode. All these curves are plotted with  $m = 1$  and  $n = 1.5$ , (solid line),  $n = 1.0$  (small dashed line) and  $n = 0.1$ , (- \* - \*). Here  $n$  quantifies the azimuthal velocity  $V_\phi^2 = nGMR_{in}/r$ .

analysis, is based on the equilibrium solution presented by us (Tripathy *et al.* 1990). The stability analysis is performed using the eigenvalue technique to solve the set of linearised equations which are Fourier transformed in the inhomogeneous direction under the local approximation. The technique was first applied to the one-dimensional case (radial perturbation with  $m = 0$ ) and it is concluded that the results agree quite well with the results obtained earlier in paper I. In addition the method illustrated the eigenmode structures of the unstable modes and revealed that the density perturbation has the maximum amplitude for a given value of the wavelength. The analysis further showed that the nature of the mode structures have the same pattern as their growth rates and hence verified the consistency of the formalism.

Next we analysed the stabilizing characteristics of the finite azimuthal mode number. The analysis revealed that out of the possible four modes, two are unstable and they are identified as fast and slow magnetosonic modes. A study of the growth rates as a function of the azimuthal ( $m$ ) and radial ( $k$ ) wave number revealed that the growth rates of these modes have higher values for higher  $m$  numbers and does not

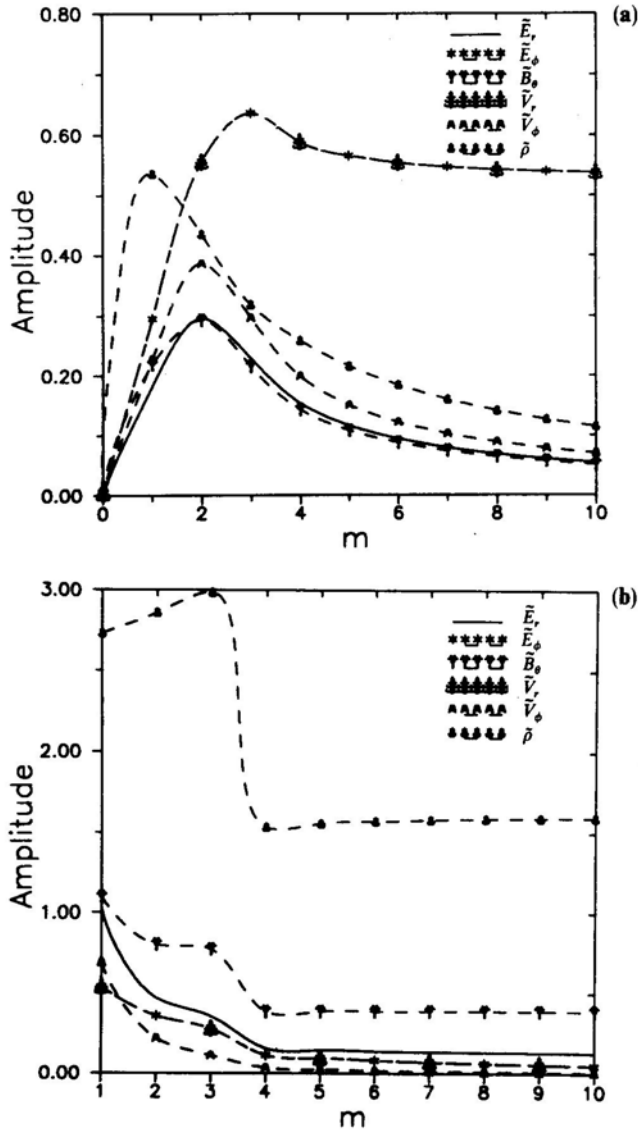


**Figure 8.** The normalised eigenmode structures of (a) FMS Mode (b) SMS mode for purely azimuthal mode ( $k = 0$ ).

change appreciably for higher  $k$  values. For a given set of disk parameters the normalised growth rate of the slow mode is found to be smaller by two orders of magnitude than the fast mode. In addition it is found that for purely azimuthal propagation ( $k = 0$ ) the growth rates of the magnetosonic modes are small and that the eigenvalue and eigenmodes have a similar structure.

The investigation carried out to analyse the effects of different parameters on these two instabilities pointed out that the growth rate of the fast mode is significantly affected by the disk parameters whereas that of the slow mode is unaffected. The study also showed the differences in the propagation and dispersion characteristics

of the magnetosonic modes. These two modes which propagate in opposite directions have contrasting dispersive characteristics. The fast mode is non-dispersive along the radial direction with resonance eigenvalue  $\omega_r \sim 0.25$  and dispersive in azimuthal direction whereas the slow wave is dispersive in radial direction and non-dispersive in azimuthal direction. The resonant eigenvalue (real) of the slow mode is a sensitive function of the plasma flow. Furthermore, the eigenmode structures have qualitatively the same pattern as the corresponding growth rate and proves the consistency of the calculation. Similar to the case of one-dimensional perturbation analysis, the magnetosonic modes are found to be independent of conductivity.

Although, our results qualitatively agree with the instability studies of earlier investigations (Anzer & Börner 1980, 1983; Miura & Pritchett 1982; Pietrini & Torricelli-Ciamponi 1989; Corbelli & Torricelli-Ciamponi 1990), we find that our results have some quantitative differences. We attribute this to the following factors. The basic difference lies in our geometry. We recall that our analysis started with the study of dynamics and structure of equilibrium configurations in relativistic formalism which adopted a spherical geometry. The same coordinate system is retained for the stability analysis. The other point to be stressed is the self-consistent equilibrium solution which involved many physical parameters compared to the equilibrium configuration adopted by others. Further, our equilibrium configurations of magnetic and velocity fields have smooth profiles in contrast to the jump conditions (either in velocity or density field) considered by the above authors. In addition, in our analysis the wave propagates along the direction of the velocity shear in contrast to the usual studies where the direction of propagation is taken transverse to the shear direction. In spite of these differences the results of our instability analysis for purely azimuthal mode ( $k=0$ ) partially coincide with the other known results.

### References

- Anzer, U., Börner, G. 1980, *Astr. Astrophys.* **83**, 183.  
 Anzer, U., Börner, G. 1983, *Astr. Astrophys.*, **122**, 73.  
 Corbelli, E., Torricelli-Ciamponi, G. 1990, *Phys. Fluids B*, **2**, 828.  
 Miura, A., Pritchett P. L. 1982 *J. Geophys. Res.*, **87**, 7431.  
 Pietrini, P., Torricelli-Ciamponi, G. 1989, *Phys. Fluids B*, **1**, 923.  
 Prasanna, A.R. 1991, *Pramana-J. Phys.*, **36**, 445.  
 Rognlien, T. D., Weinstock, J. 1974, *J. Geophys. Res.*, **79**, 4733.  
 Simonutti, M. D. 1976, *Phys. Fluids*. **19**, 636.  
 Smith, B. T., Boyle, J. M., Garbow, B. S., Ikobe, Y., Klema, V. C, Moler, C. B. 1974, *Lecture Notes in Computer Science*, **6**, Springer Verlag, Berlin.  
 Tripathy, S. C, Prasanna A. R., Das, A. C. 1990, *Mon. Not. R. astr. Soc*, **246**, 384.  
 Tripathy, S. C, Dwivedi, C. B., Das, A. C, Prasanna, A. R. (paper I) 1993, *J. Astrophys. Astr.*, **14**, 103.